

AP-A138 945

INTRODUCTION TO THE LASER-HANE EXPERIMENT AND SUMMARY
OF LOW-PRESSURE INTERACTION RESULTS(U) NAVAL RESEARCH
LAB WASHINGTON DC B H RIPIN ET AL. 22 FEB 84

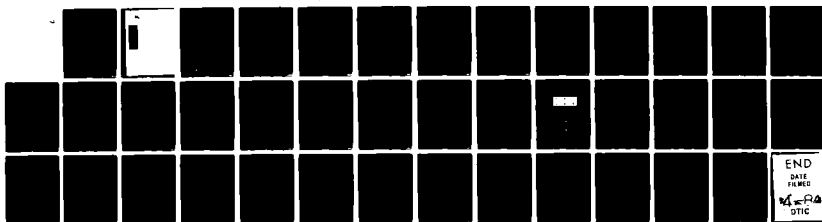
1/0

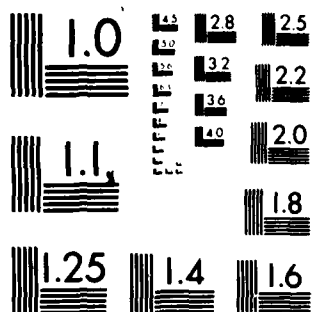
UNCLASSIFIED

NRL-MR-5268

F/G 20/5

NL





MICROCOPY RESOLUTION TEST CHART
NATIONAL BUREAU OF STANDARDS 1963-A


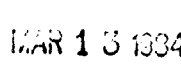

AD A1 38945

REPORT DOCUMENTATION PAGE				
1a. REPORT SECURITY CLASSIFICATION UNCLASSIFIED			1b. RESTRICTIVE MARKINGS	
2a. SECURITY CLASSIFICATION AUTHORITY			3. DISTRIBUTION/AVAILABILITY OF REPORT	
2b. DECLASSIFICATION/DOWNGRADING SCHEDULE			Approved for public release; distribution unlimited.	
4. PERFORMING ORGANIZATION REPORT NUMBER(S) NRL Memorandum Report 5268			5. MONITORING ORGANIZATION REPORT NUMBER(S)	
6a. NAME OF PERFORMING ORGANIZATION Naval Research Laboratory		6b. OFFICE SYMBOL (If applicable)		7a. NAME OF MONITORING ORGANIZATION
6c. ADDRESS (City, State and ZIP Code) Washington, DC 20375			7b. ADDRESS (City, State and ZIP Code)	
8a. NAME OF FUNDING/SPONSORING ORGANIZATION Defense Nuclear Agency		8b. OFFICE SYMBOL (If applicable)		9. PROCUREMENT INSTRUMENT IDENTIFICATION NUMBER
8c. ADDRESS (City, State and ZIP Code) Washington, DC 20305			10. SOURCE OF FUNDING NOS.	
11. TITLE (Include Security Classification) (See page ii)			PROGRAM ELEMENT NO. 62715H	PROJECT NO. 47-1606-0-4
12. PERSONAL AUTHOR(S) B.H. Ripin, J. Grun, S. Kacenjar, E.A. McLean, and J.A. Stamper			TASK NO.	WORK UNIT NO.
13a. TYPE OF REPORT Interim	13b. TIME COVERED FROM _____ TO _____		14. DATE OF REPORT (Yr., Mo., Day) February 22, 1984	15. PAGE COUNT 39
16. SUPPLEMENTARY NOTATION This research was sponsored by the Defense Nuclear Agency under Subtask I25BMXIO, work unit 00024 and work unit title "Early Time Plasma."				
17. COSATI CODES			18. SUBJECT TERMS (Continue on reverse if necessary and identify by block number)	
FIELD	GROUP	SUB. GR.	HANE Laser-plasma Shocks	
			Instabilities Magnetized ion-ion	
19. ABSTRACT (Continue on reverse if necessary and identify by block number)				
<p>A brief overview of the NRL laser-target experiment which simulates the interactions involved in a HANE is presented. A burst of fast laser-produced-debris-ions stream into a low-density magnetized ambient plasma/gas. The interactions between these two plasma components are investigated under a variety of conditions.</p> <p>At ambient pressures below 150 mTorr we observed a magnetic bubble formation during the debris expansion; we found that the field is swept out of the volume traversed by the debris plasma and is compressed ahead of the debris front. Evidence is found for magnetic-field dependent interactions between the debris ions and ambient plasma.</p>				
20. DISTRIBUTION/AVAILABILITY OF ABSTRACT UNCLASSIFIED/UNLIMITED <input checked="" type="checkbox"/> SAME AS RPT <input type="checkbox"/> DTIC USERS <input type="checkbox"/>			21. ABSTRACT SECURITY CLASSIFICATION UNCLASSIFIED	
22a. NAME OF RESPONSIBLE INDIVIDUAL B. H. Ripin			22b. TELEPHONE NUMBER (Include Area Code) (202) 767-2730	22c. OFFICE SYMBOL Code 4732

DD FORM 1473, 83 APR

EDITION OF 1 JAN 73 IS OBSOLETE.

SECURITY CLASSIFICATION OF THIS PAGE

11. TITLE

INTRODUCTION TO THE LASER-HANE EXPERIMENT AND SUMMARY OF LOW-PRESSURE
INTERACTION RESULTS

CONTENTS

I. INTRODUCTION	1
II. EXPERIMENT AND DIAGNOSTICS	2
III. SCALING OF LASER-EXPERIMENT TO HANE	5
IV. LOW-PRESSURE AMBIENT-PLASMA REGIME	7
V. COLLISIONLESS INSTABILITY REGIME	9
VI. SUMMARY	11
VII. ACKNOWLEDGMENTS	12
REFERENCES	25



[Faint, mostly illegible text and a signature are visible in the bottom right corner of the page.]

INTRODUCTION TO THE LASER-HANE EXPERIMENT AND SUMMARY OF LOW-PRESSURE INTERACTION RESULTS

I. Introduction

DNA's Division of Atmospheric Effects (RAAE), initiated a laser-target HANE-simulation experiment at the Naval Research Laboratory in early 1982. The objective of this experiment is to study the mechanisms involved in a HANE event, especially those which affect the early-time evolution of the plasma structure.⁽¹⁾ The experiments have two goals. The first objective is to emulate a nuclear event as closely as possible. Laboratory parameters which cannot directly duplicate those of a real or hypothetical HANE, such as masses and distances, have to be scaled using an appropriate scaling argument. The second goal is to study relevant physical effects or mechanisms, even if the experimental parameters are quite far from that of a direct simulation. In either case coupling to the theoretical activity in the HANE-community is desirable to achieve a better understanding of the consequences of a HANE-like event and its relationship to the laboratory findings.

The experiment to date has focused on three regimes of interest. These are:

- o Collisionless Coupling Regime (low ambient pressure).
- o Collision Dominated Regime (high ambient pressure).
- o Disassembly Regime (high debris density, high debris acceleration).

The collisionless coupling (or low-pressure) regime is used to address the mechanisms involved in the debris-air coupling at high-altitudes (such as in Starfish), where collisionless or Longmire coupling is operative; a review of our experiments in this regime forms the major portion of this and the next paper.⁽²⁾

Manuscript approved November 29, 1983.

When ambient gas pressure is above a few-tenths of torr (high-pressure), the experiment exhibits collisional characteristics that correspond to HANE conditions in the 100 to 200 km altitude range (such as Checkmate). Our first experiments in this regime is the subject of several other papers in this proceedings.^(3,4,5)

Finally, the disassembly regime is concerned with the nonuniformities that may result during the detonation stage when the weapon material is highly accelerated outward by the released energy; a primary question is whether these nonuniformities grow due to Rayleigh-Taylor instability⁽⁶⁾ and evolve into later-time structure.⁽⁷⁾ Experiments addressing this subject are the subject of another paper in this proceedings.⁽⁸⁾

II. Experiment and Diagnostics

I will now outline the configuration of the present experiment and the parameter regimes that are accessible. Enhancements to the laser and target facility presently being made will also be briefly described.

The experiment involves focusing beams from the NRL-Pharos II Nd-laser (1.05 μm wavelength) onto a small ($< 1 \text{ mm}$ dia, few-microns thick foil) solid target in the center of the target chamber. Target material is ablated by the laser irradiation and streams radically outward with kinetic energy densities comparable to those resulting from a weapon detonation. A low-density background gas in the chamber is promptly ionized near the target by radiation from the laser-target interaction (photoionization), and at later times by the expanding debris (UV photoionization from the debris shell or by particle impact). This creates an ambient plasma, through which the high-velocity nuclear-like debris streams, emulating the ionospheric conditions surrounding a detonation; an external magnetic field can be applied over the whole interaction

region, using permanent magnets or coils, to mock-up the ionospheric magnetic field. As we will see, with appropriate scaling the spatial dimensions of the relevant interaction region is of the order of centimeters, the time-scales involved are fractions of a microsecond, the magnetic fields are close to kilogauss and the required ambient gas pressure is below ten Torr (1 Torr = 1 mm of Hg = 3.24×10^{16} molec/cc). The laser-pulse energy requirement to simulate a detonation is also reasonable, being 10 to 1000 Joules. Figure 1 shows the experimental arrangement schematically. Some of the present and (to be) upgraded facility specifications are tabulated in Table I. The facility upgrade, which includes extensive modifications to both the laser and the target areas, is expected to be completed in late FY-84 or early FY-85.

Table I. Facility Specifications

	LASER			CHAMBER/GAS		MAGNETIC FIELD	
	Energy ^(a) (J)	λ (μ m)	#Beams	Diameter (cm)	P ^(b) (Torr)	B(kgauss)	Coil Diameter (cm)
Present	400	1.05	2 ^(c)	60	$> 10^{-5}$	0.8 ^(d) 0-1 ^(e)	5 10
Upgrade	1500	1.05 ^(f) 0.53 ^(f)	3 ^(g) 2-3	130	$> 10^{-6}$	0-10 ^(e)	26

(a) In a 3-4 nsec pulse; a 300 psec pulse duration is also available at reduced total energy

(b) Any gaseous species

(c) One-sided illumination

(d) Permanent magnet

(e) Helmholtz and dipole coil configurations

(f) Narrow or broad bandwidth laser pulse

(g) One or two-sided illumination

Many diagnostics are available to measure the evolution of the debris-plasma interaction; and others are currently being developed.⁽⁹⁾ Diagnostics include devices to measure: the incident and reflected laser energy and time-history, the angular distributions of the resulting debris energy, velocity,

mass, and momentum. Magnetic probes measure the magnetic field distortions during the debris/background plasma interactions and self-generated magnetic field components as a function of position and time. Electric probes give similar information about the electric field and plasma properties in low-density plasma. Optical diagnostics such as shadowgraphy and interferometry yield quantitative pictures of the plasma density structure at moderate-to-high densities ($> 10^{17}$ electrons per cm^3) optical imaging with still-photography, time-resolved framing photography, or streak photography also give qualitative and quantitative information on density structure. Spectroscopy, from the infrared to XUV, is used to give spatially and temporally resolved information about the velocity, temperature, ionization state, density, emissivity, opacity, etc. of the debris material, the photoionized background plasma, and the interaction between them. Ion analyzers (under development)⁽¹⁰⁾ will allow measurements of the debris and reflected ambient ion velocity and species distributions along and across the magnetic field. Knowledge of the ion properties is valuable in resolving many of the current questions about early-time HANE instabilities. X-ray and XUV diagnostics allow diagnosis of plasma properties above about 20 eV; pinhole or imaging photography gives 2-D spatially-resolved images while electronic x-ray and UV detectors give quantitative information about the initial debris plasma temperature, the UV emission from the expanding debris-ambient plasma front, etc. Still other novel techniques are used for specific information. Tracer-dot techniques, in which small dots of a high-Z material are implanted in the target surface, have proved valuable in providing debris flow visualizations and spatially resolved quantitative spectroscopy.⁽¹¹⁾ Resonant and nonresonant laser scattering in the disturbed plasma has been proposed to measure the density power spectrum.⁽¹²⁾ The experiment can also provide a short-pulse x-ray flash for quantitative x-ray

radiography of the highly-accelerated ($> 10^{15}$ cm/sec²), high-density (> 0.1 solid) targets in the accelerating target regime.⁽¹³⁾ Highly accelerated targets, which can be purposefully structured, are being used to study the hydrodynamic stability of material during device disassembly and the sensitivity of plasma structure evolution to nonuniformities in the target.⁽¹³⁻¹⁶⁾

III. Scaling of Laser-Experiment to HANE:

Scaling of HANE-parameters down to laboratory conditions is predicated on several alternate sets of assumptions, depending upon the physics of interest. No set of assumptions will simultaneously reproduce all aspects of a HANE event; one should, therefore, consciously choose which physical conditions are to be retained on the basis of their importance to the experiment. Longmire formalized one scaling scheme by fixing the debris velocity in the laboratory experiment to be equal to that of a real HANE and by preserving binary collisions;⁽¹⁷⁾ this scaling preserves binary collision effects but not magnetic field and plasma instability effects. It is a reasonable approach when details of collisions are crucial. Also, it gives a feeling for how parameters scale from a HANE down to the laboratory. Table II shows Longmire collisional scaling relations as a function of the yield ratio $Y \equiv E_d/T_w$ between the HANE-weapon and laboratory debris kinetic energies. As mentioned before, most of these parameters are achievable in the experiment. But, if the focus of a particular investigation is the role of streaming instabilities for "collisionless" debris-air momentum transfer,⁽¹⁸⁾ other scaling relations are more appropriate. Scalings which emphasize instability coupling have been discussed by ourselves⁽¹²⁾ and, more thoroughly, by Tsai, DeRaad and Lelevier (RDA),⁽¹⁹⁾ Smith and Huba (NRL),⁽²⁰⁾ Stellingwerf, Longmire and Alme (MRC),⁽²¹⁾ and Sperling (JAYCOR).⁽²²⁾ These scalings generally relax the debris velocity and

material constraints but require stronger magnetic fields than strict B^2/nkT scaling. The parameters of the target facility upgrade were, in fact, chosen to allow clean studies of this type. Undoubtedly, other phenomena of interest, such as MHD-EMP, highly-accelerated dense material, etc., require still other scaling emphasis.

The targets can be irradiated in three modes: the exploding-pusher mode; the ablation mode; and the accelerating target mode. The exploding pusher mode⁽²³⁾ occurs at high laser irradiance and yields very high-velocity ion debris (but with a broad nonreproducible distribution). The ablation mode^(24,25) occurs at lower laser irradiance ($I < 10^{14}$ W/cm²) and yields a very reproducible narrow ($\Delta v/v \approx \pm 0.1$) ion velocity distribution with mean velocity tunable between 10^7 and 8×10^7 cm/sec. This mode of operation is particularly suitable for detailed HANE investigations due to its simplicity, reproducibility, and cold ion distribution; this is the mode of preference for most studies. The third mode, the accelerating target mode,^(14,24,25) uses the ablating debris to accelerate a thin target to high-speed (up to 2×10^7 cm/sec) while remaining near solid-density (> 0.1 solid density) and cold (< 10 eV). Each of these modes can be exploited for specific HANE studies.

The laser-plasma interaction can deposit energy densities comparable to those of a real weapon and set up conditions close to (but not identical to) actual HANE-events. The time and spatial scales are experimentally achievable and well-diagnosed experiments can be done in a repeatable and repetitive manner at modest cost (comparatively speaking). Therefore, with your help many issues crucial to HANE phenomenology and structure evolution will soon be tested.

A brief description of our exploratory experiments in the low-pressure or collisionless regime follows. We search for signs of a collisionless mechanism such as plasma instability that could couple the debris momentum to the ambient

Table II. Collisional (Longmire⁽²⁾) scaling of selected HANE parameters with the relative energy ratio Y .

<u>Parameter</u>	<u>Scaling</u>	<u>Representative values for $Y=10^{-12}$</u>
Velocity	$v = \text{constant}$	10^8 cm/sec
Mass (debris)	$m_d \propto Y$	0.1-1 μgm
Distances	$R \propto Y^{1/2}$	~ 1 cm
Time	$t \propto Y^{1/2}$	~ 100 nsec
Background density gas	$p \propto Y^{-1/2}$	10^{13} - 10^{18} atoms/cc
*Magnetic field	$B \propto Y^{-1/4}(a); Y^{-1/2}(b)$	~ 1 kG (a); ~ 1 MG (b)
*MII instability	$\gamma\tau \propto Y^{1/4}(a); \text{const}(b)$	~ 1 (a); $\sim 10^3$ (b)

*The magnetic field does not scale uniquely. The (a) scaling preserves the magnetic field/plasma energy density ratio (B^2/nkT) which also preserves the Alfvén velocity constant; in this scaling the number of instability growth times is compromised. An alternate assumption (b) is to keep Larmor radii constant with other distance scales; this requires unrealistically high magnetic field.

IV. Low-Pressure Ambient-Plasma Regime

In our first experiments in the low-pressure (< 150 mTorr) regime, we search for signs of beam-plasma instabilities. These instabilities are thought to effect debris-air coupling in high-altitude events, such as in Starfish (400 km), in which collisions alone are insufficient to transfer momentum from the device debris to the ionosphere. The experimental configuration and the ambient and debris ion velocity distributions are sketched in Fig. 2. Of the five streaming instabilities thought to be relevant to HANE (Lampe et al.)⁽¹⁸⁾ we focus our attention on the magnetized ion-ion instability. The magnetized ion-ion instability is an efficient momentum transfer mechanism with an effective collision frequency of about one-tenth the lower hybrid frequency.

We are in a regime in which the debris ions are unmagnetized (cyclotron radius \gg equal mass radius), the ambient plasma is magnetized (electron and ion cyclotron radii $<$ the equal mass radius) and, most importantly, the debris

magnetic Mach number is high ($V_D > V_{\text{Alfven}}$). The latter constraint is deemed important to preserve the hydrodynamics of a HANE event.

The uncoupled debris ion distribution has high-velocity (up to 8×10^7 cm/sec) and a narrow spread ($\pm 10\%$) as seen in the typical time-of-flight detector signal of Fig. 3. The first blip is the $t=0$ marker (due to the x-ray flash from the laser-target interaction; this occurs on this plot at about 0.4). The mean velocity of the ions is 6×10^7 cm/sec in this case. The debris-ion distributions are well-behaved and reproducible in the absence of an interaction. Moreover, they can be tuned up or down in velocity by changing the laser irradiance.⁽²⁵⁾ The relative velocity between debris and ambient ion distributions exceeds the thermal spreads of the beams, thus satisfying the criteria for streaming instability.

When ambient gas is present, the debris distributions are altered. For ambient pressures of 80 millitorr and up, the debris ion distributions reaching the time-of-flight detector (about 22 cm away from the target) are attenuated and slightly broadened, as in Fig. 4. These changes to the debris velocity distributions are thought to be due to collisional processes, or at least magnetic field independent mechanisms, since they do not seem sensitive to the presence or absence of a magnetic field (at least not sensitive to fields below one-kilogauss).

To test the collisional properties of the debris ions in traversing tens-of-centimeters of ambient plasma and gas before detection, we use the setup shown in Fig. 5. Three time-of-flight charge collector detectors are placed at 10 cm, 25 cm, and 55 cm distances from the target to detect ion distribution changes occurring between them.

One question is whether we can rely upon the preservation of the shape of the ion distribution in passing through the ambient media; if so we can detect

the effects of an interaction occurring within a few centimeters of the target much further away. The answer is seen in Fig. 6; at least through a mass-pathlength of 5×10^{16} molecules/cc * cm (i.e., 150 mTorr N_2 with $l = 10$ cm) both the peak velocity and velocity spreads are not strongly affected. Therefore, they can be used as good indicators of interactions close to the target.

Another related question is whether significant debris ion charge is being lost due to charge exchange processes between the target and detector. Figure 7 shows that the answer is affirmative for low-velocity carbon debris (< 350 km/sec) for mass-pathlengths above about 10^{16} molecules/cm², and for higher velocity Al at somewhat higher pressures. Thus, the attenuation of debris ions exhibited in Fig. 4 could be due to charge exchange or ion removal type processes.

Nonetheless some energy, albeit a small amount, is transferred from the debris to an expanding shell in the 100 mTorr regime; this is seen in the framing camera pictures of visible light emission, Fig. 8. A fuzzy shell expands with a speed of about 250 km/sec into a 100 mTorr N_2 background gas in which an 800 G external field was applied. Measurements of the magnetic field dynamics show that the ambient field is largely swept out of the region traversed by the debris and is compressed ahead of the debris front, as illustrated in Fig. 9. An extensive description of the magnetic field behavior is to be found in a paper by Kacenjar et al.⁽²⁾ elsewhere in this proceedings.

V. Collisionless Instability Regime

For what experimental parameters is the magnetized ion-ion instability most likely to be observed? To answer this question we examine the instability criteria outlined in Lampe et al.⁽¹⁸⁾ To satisfy the two most stringent

instability criteria, that of avoiding electromagnetic stabilization ($V_D/V_A \equiv M_A \lesssim 2.5$) and fitting at least one parallel wavelength in the system size ($\lambda_{||} < 2\pi R_m$), we should go in the direction of:

- o Increasing the magnetic field
- o Decreasing the ambient density
- o Decreasing the drift velocity
- o Decreasing the atomic number of the ions.

Smith and Huba quantitatively outlined expected regions of instability in laser energy-ambient pressure space, as shown in Fig. 10. For example, Figure 11 shows that carbon debris interstreaming through an 800 G magnetized ambient hydrogen plasma at a velocity of 400 km/sec should be MII unstable close to the experimentally accessible circled region. The outlined regions of instability assume full ionization of the hydrogen and therefore would move to the right in Fig. 10 if the gas is partially ionized (as indeed it is).

To detect the presence of instability, an array of four charge time-of-flight detectors is deployed perpendicular to the magnetic field direction but at various angles from the target normal, as sketched in Fig. 12.

A clear difference between the debris ion distributions with and without the magnetic field in place is seen in Fig. 13. Without a field present, as in the ion distributions on the left side of Fig. 13, the debris distributions are well-behaved and similar to those generated in a vacuum. In contrast, the distributions in the presence of the magnetic field (on the right) are broadened and have lower velocity (later-time) peaks which are like signatures of expected beam-plasma instability. The pressure is low and collisions play little or no role.

We used hydrogen gas to have a low the ambient-plasma atomic number in order to be more susceptible to instability, as indicated previously. To test the conjecture that lower atomic number is more unstable we compared debris ion distributions resulting from use of nitrogen ($A=28$) and hydrogen ($A=1$), as shown in Fig. 14. The magnetic field dependent interaction that occurring in hydrogen is not evident in nitrogen. This lends support to the notion that MII may be occurring in the carbon-hydrogen combination but not in carbon-nitrogen under our conditions.

Finally, sometimes ion signals are observed with components having higher velocities than in the original debris distributions. This occurs (for example in the circled regions of Fig. 15) at low incident laser energy in cases which exhibit the other signs of magnetic field dependent interaction. We have very few cases of this sort, and therefore the results are considered tentative. But, these "fast ions" may be the result of a reflection or acceleration process near the coupling region.

VI. Summary

The laser-target HANE-simulation experiment can examine physics questions relevant to HANE early-time phenomena in three regimes: the collisionless (low-pressure) regime, the collisional (high-pressure) regime, and the disassembly (dense high-acceleration) regime.

In the collisionless regime, the results of the first series of experiments show magnetic field dependent interactions between the debris ions and ambient plasma. In many ways these observations are similar to those expected from the magnetized ion-ion instability. However, an extensive study of collisionless plasma instability coupling awaits the upgraded laser and target facility.

VII. Acknowledgments

This work was supported by the Defense Nuclear Agency. The authors thank Drs. W. Ali, H. Griem, M. Herbst, C.K. Manka, and S. Obenschain for their contributions to this work. Guidance from Drs. J. Huba and R. Smith has proved valuable. Also, the assistance from Mr. E. Turbyfill, N. Nocerino, K. Kearney, and Ms. B. Sands is appreciated.

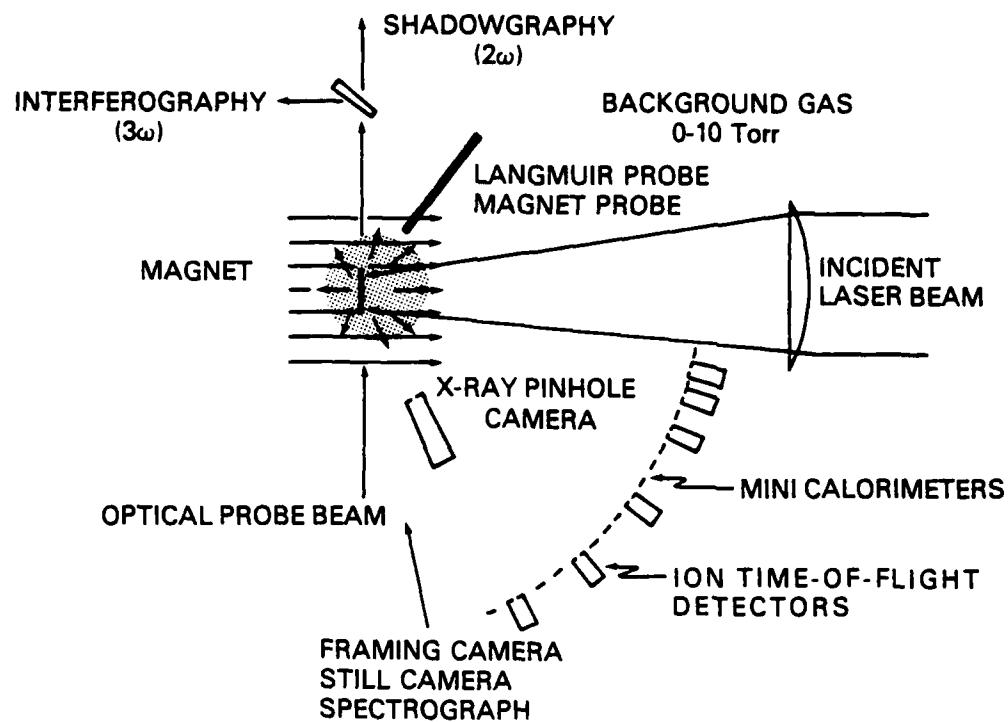


Figure 1 Experimental arrangement.

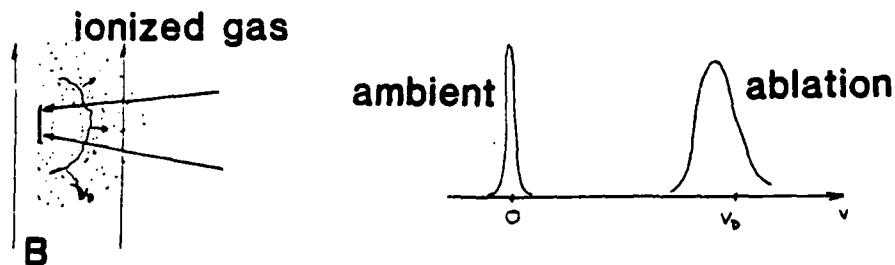


Figure 2 Schematic of the debris shell moving outward from the laser focal region through the magnetized photoionized ambient gas (left). The ambient (stationary) plasma and drifting target debris (ablation) plasma distributions form a classic interstreaming instability configuration (right).

ION TIME OF FLIGHT IN VACUUM

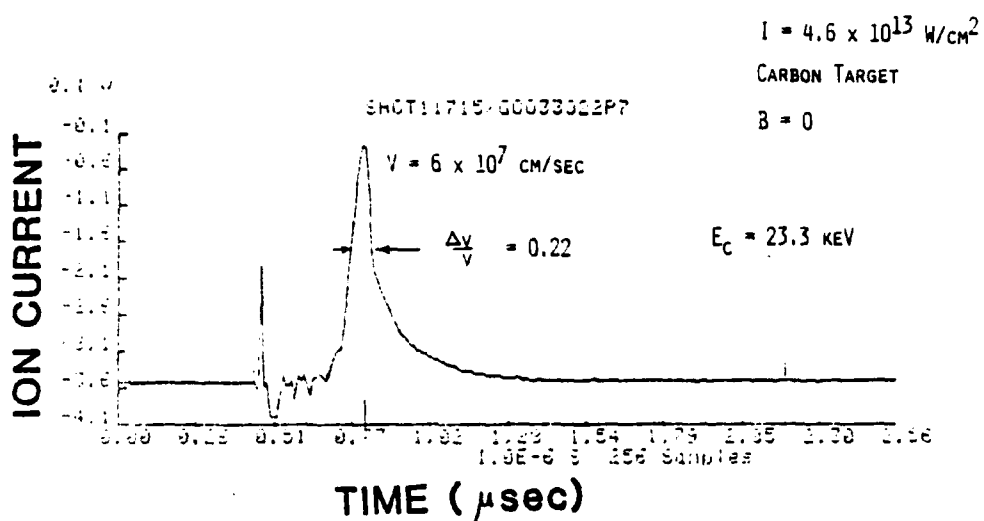


Figure 3 Debris ion time-of-flight detector signal. Note the high-velocity, narrow-velocity spread debris peak. These ions contain over 80% of the absorbed laser energy.

ION CURRENT

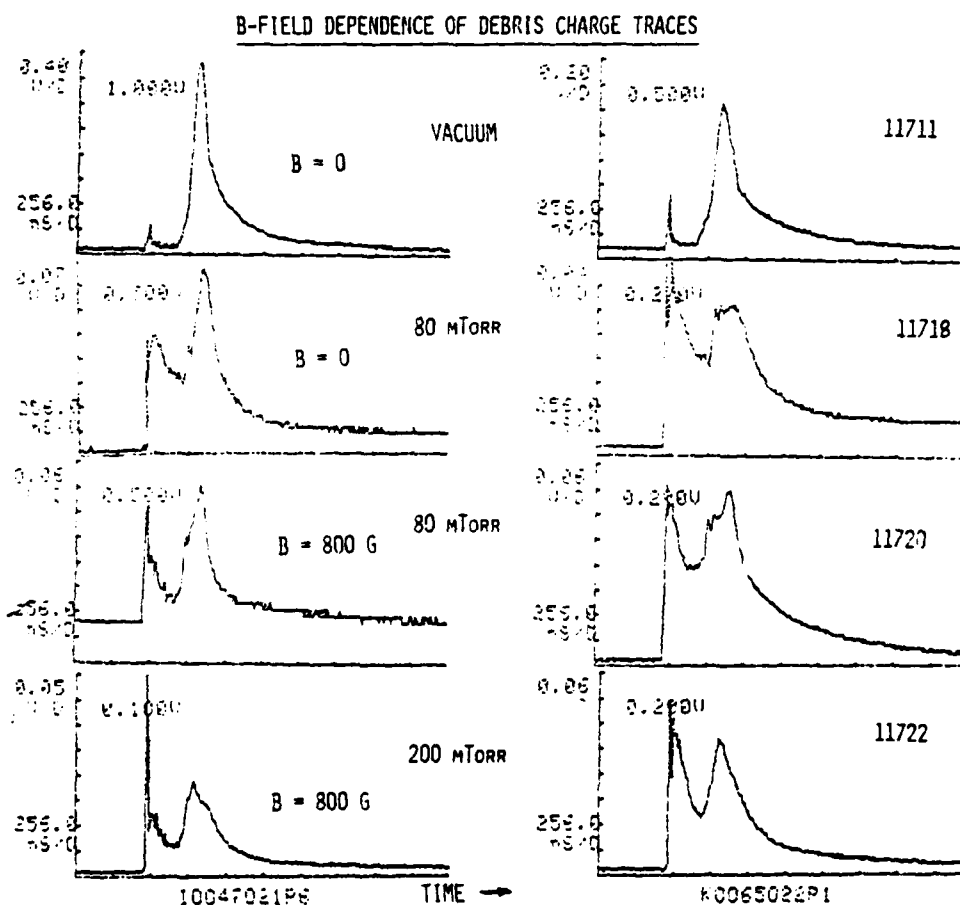


Figure 4 Debris ion time-of-flight data for moderate pressures (vacuum, 180 and 200 mTorr nitrogen), with and without a magnetic field. Traces on the left were obtained with detectors oriented at 47° to the laser beam axis and those at the right at 65° . Detectors were about 22 cm from the target and in a plane perpendicular to the magnetic field direction.

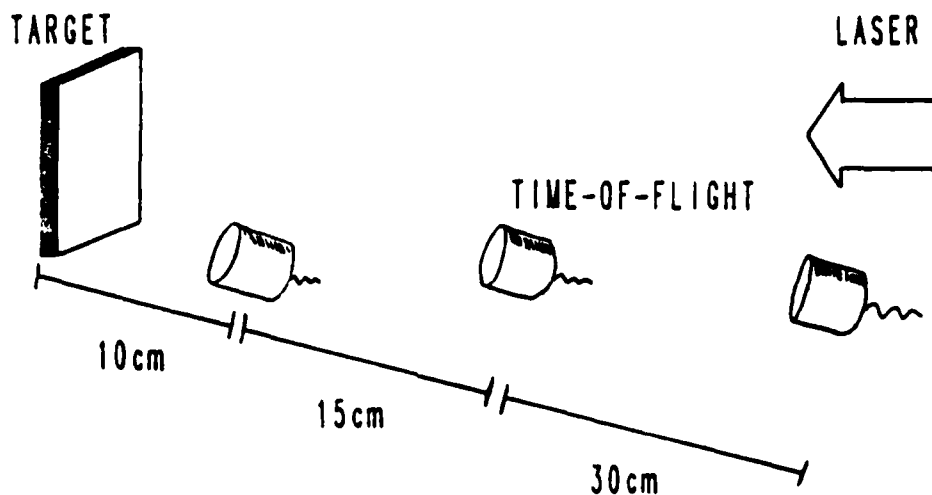


Figure 5 Setup to test the collisional properties of debris ions.

CURRENT vs AREAL DENSITY

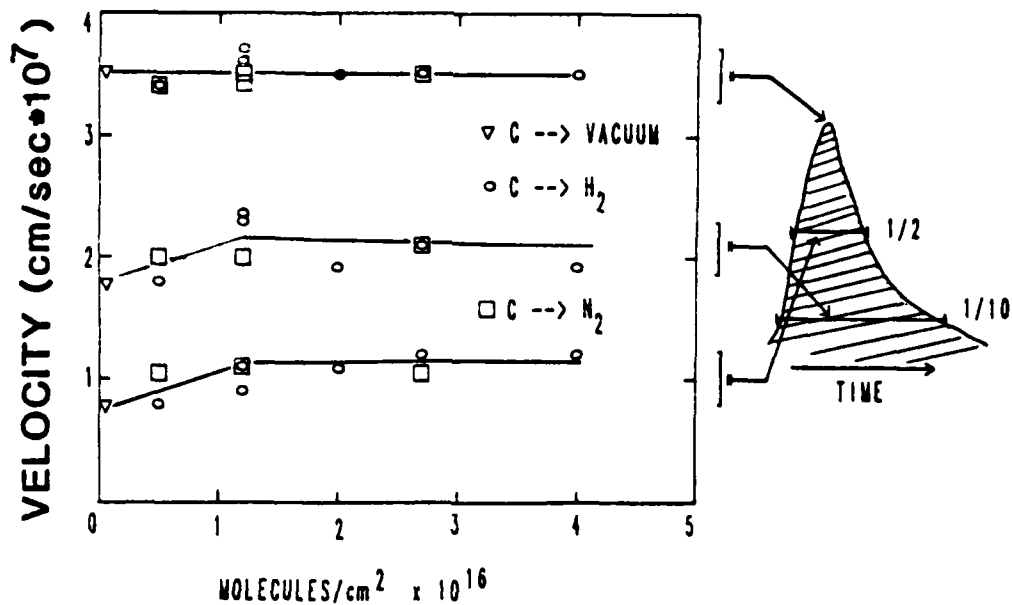


Figure 6 Peak-velocity and velocity spread (FWHM and $\pm 10\%$ points) versus mass path length of debris ions. No significant change in these ion trace characteristics are seen below 5×10^{16} molecules/cm².

CHARGE vs AREAL DENSITY

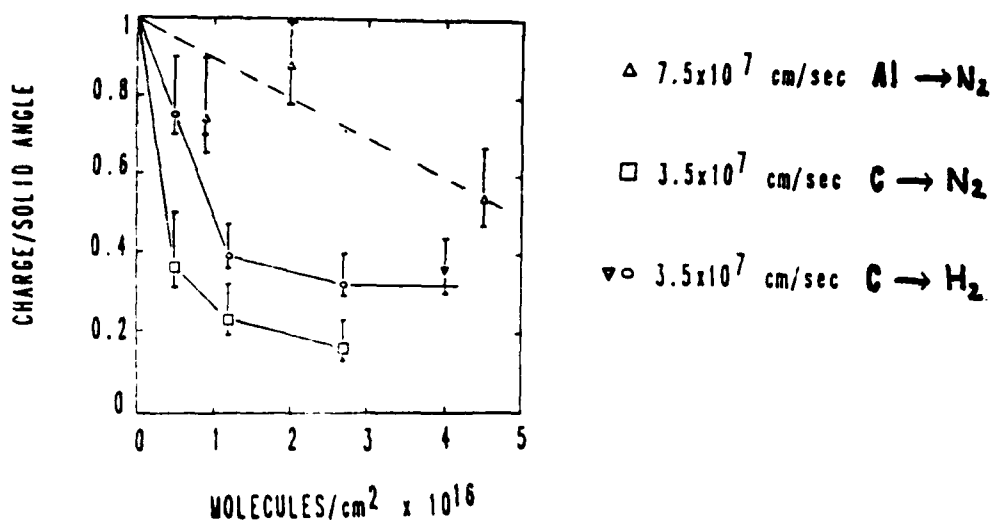


Figure 7 Debris ion charge per steradian (relative units) collected at various mass-pathlengths for several combinations of debris species and velocities and ambient gas parameters. Significant loss of charge is seen above 10^{16} molecules/cm² at low velocity.

VISIBLE FRAMING PHOTOGRAPHS

SHOT 12531
139 J, 4.5 micron Al target
100 microns Nitrogen, B=800 Gauss

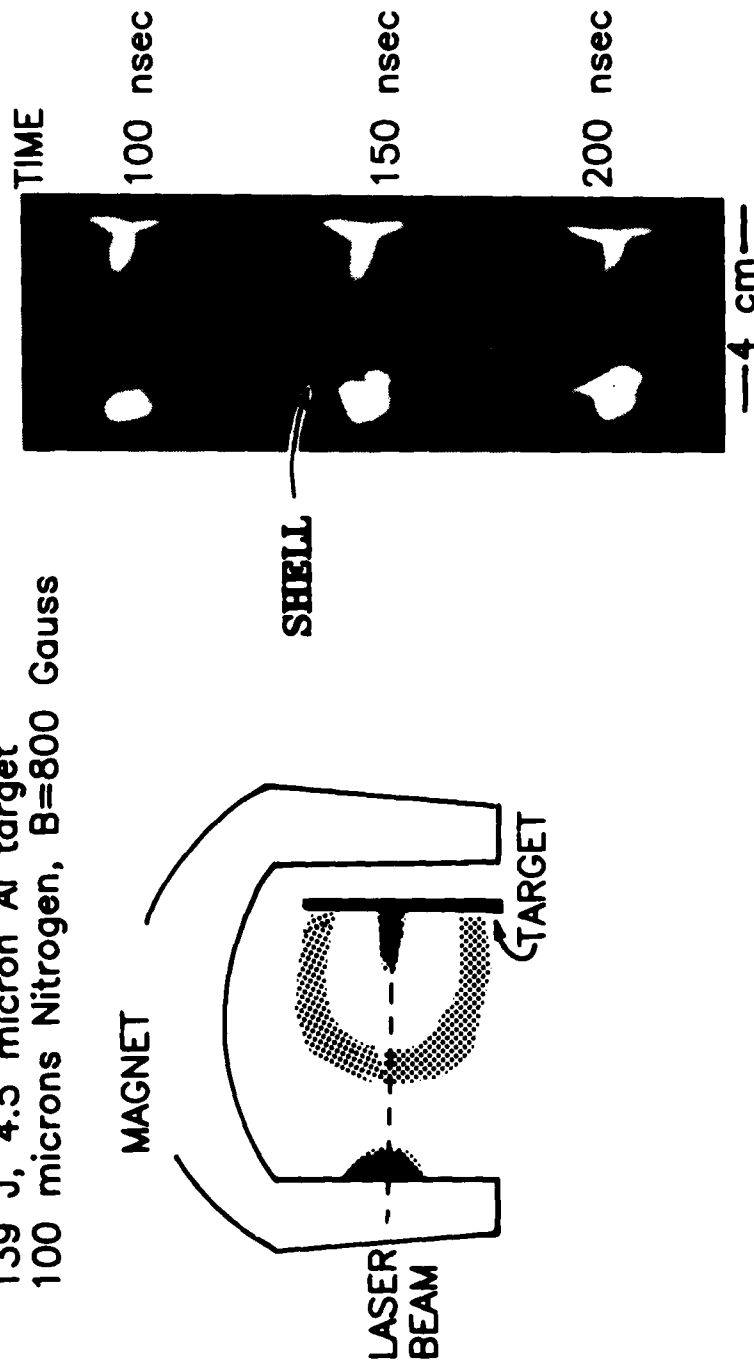


Figure 8 Framing photographs of the visible light emission from an expanding plasma shell. Frame exposure times are 5 nsec. Initial debris speed was about 6.6×10^7 cm/sec; shell speed is 2.5×10^7 cm/sec.

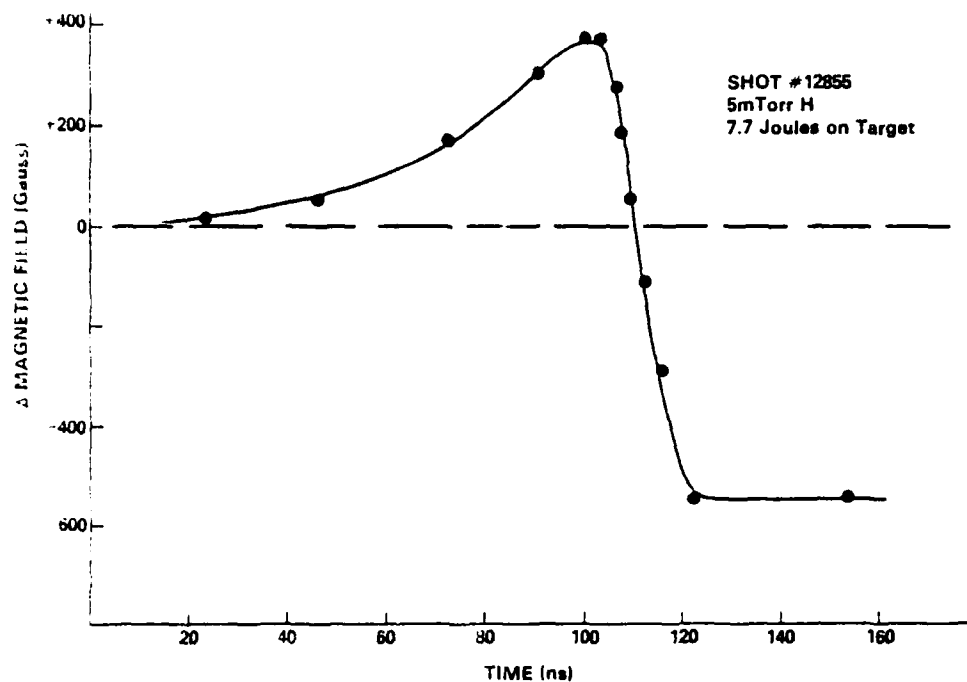


Figure 9 Temporal behavior of the change in magnetic field detected by a magnetic loop probe located 3 cm from the target. The applied field was 800 gauss. Note the field compression peak at 100 nsec and near depletion of the applied field (magnetic bubble) for $t > 120$ nsec.

TYPICAL INSTABILITY (M II)

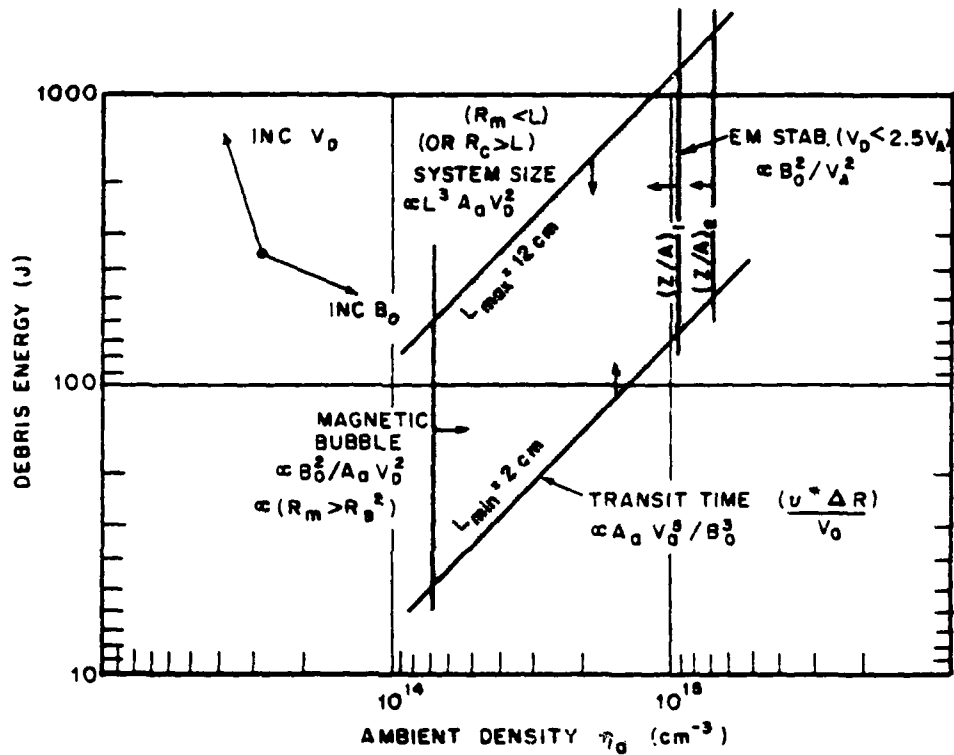


Figure 10 Magnetic ion-ion instability window (qualitative). The unstable region is bounded on the right by electromagnetic stabilization when $V_D > 2.5 V_A$, on the left by the requirement that the energy density in the debris plasma exceed that of the magnetic field, on the bottom by requiring that the transit-time of an ambient ion passing through the shell exceed one momentum transfer e-fold, and bounded on the top by the practical requirement that the equal mass radius fit inside the experiment. The top can also be limited by the cyclotron radius of the debris ions at high field strengths.

MI INSTABILITY

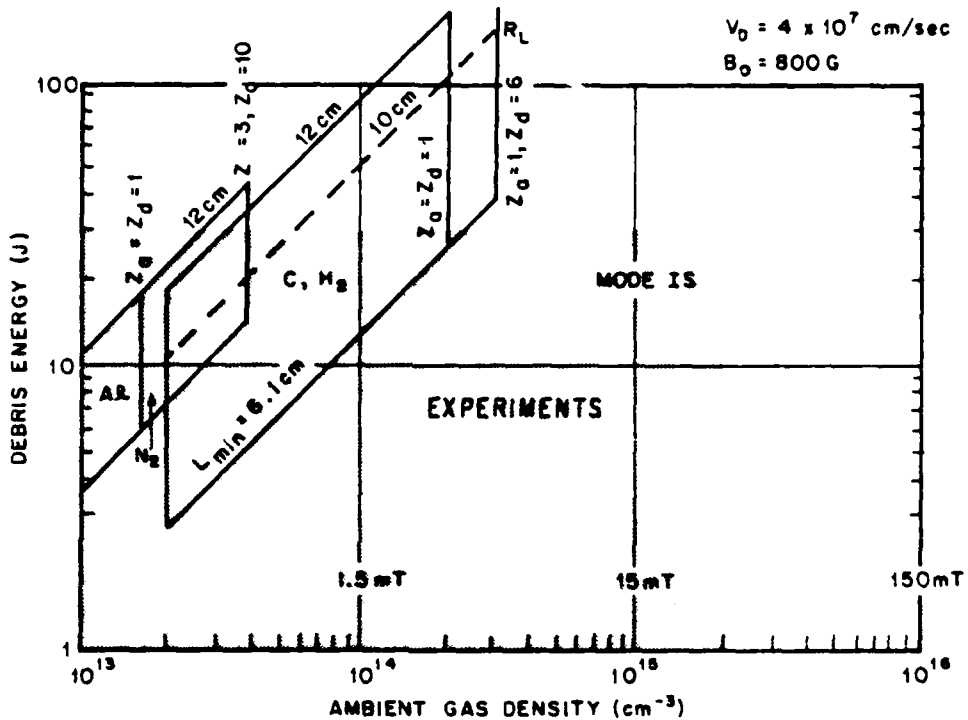


Figure 11 Parameter space for MII instability. The parallelograms are theoretical estimates of regions of instability and the circled area is the experimental region.

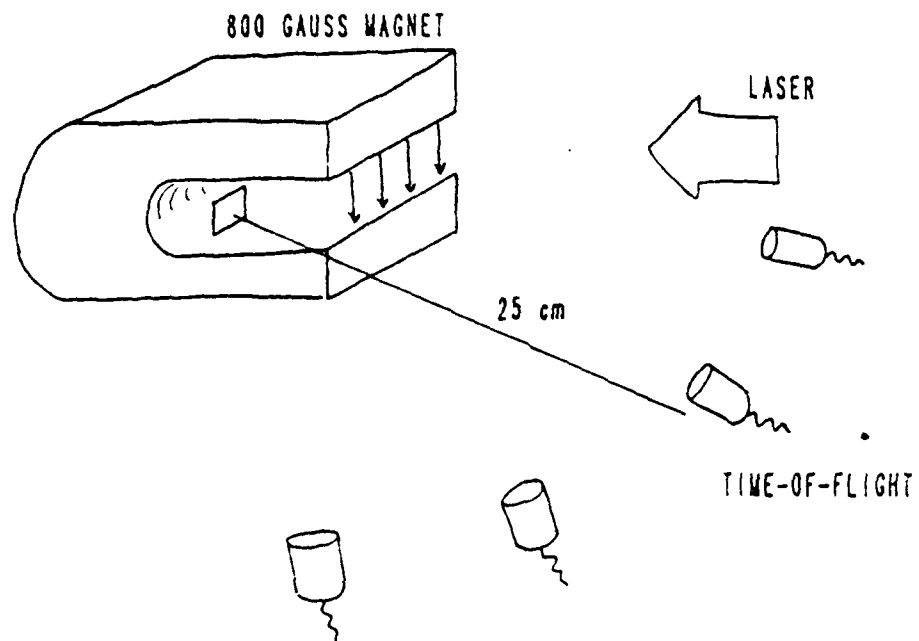


Figure 12 Arrangement to observe effects of magnetic field induced instability from debris ion time-of-flight detectors.

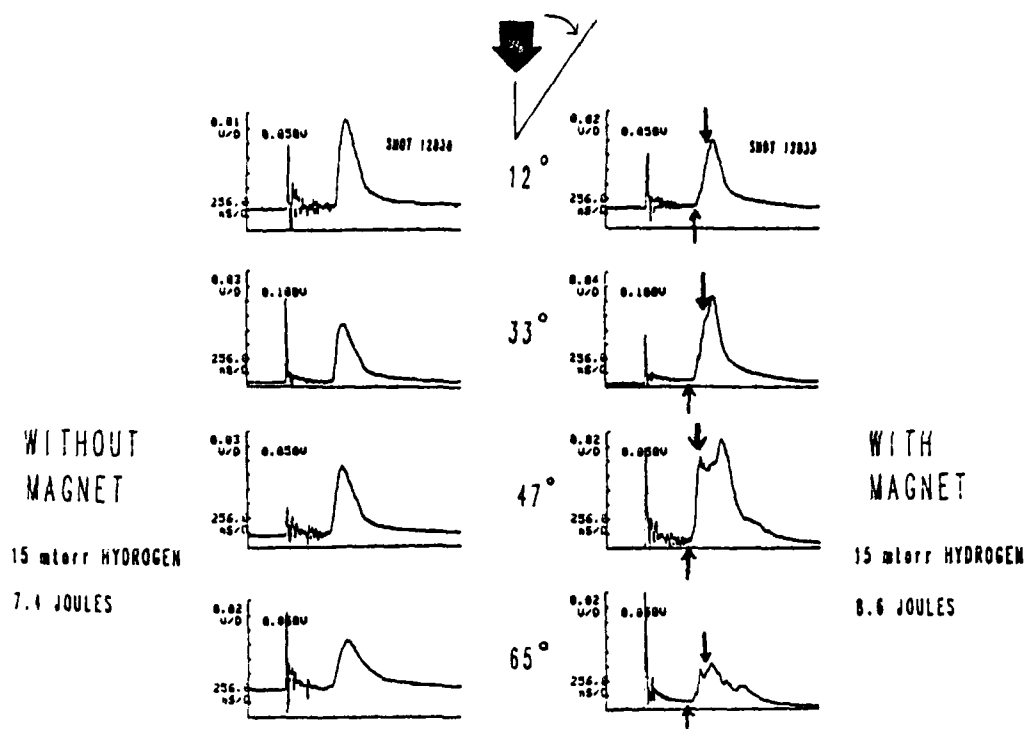


Figure 13 Comparison of debris ion time-of-flight traces without a magnetic field present (left) and with a 800 G field present (right). Note the distorted debris distributions in the presence of a magnetic field.

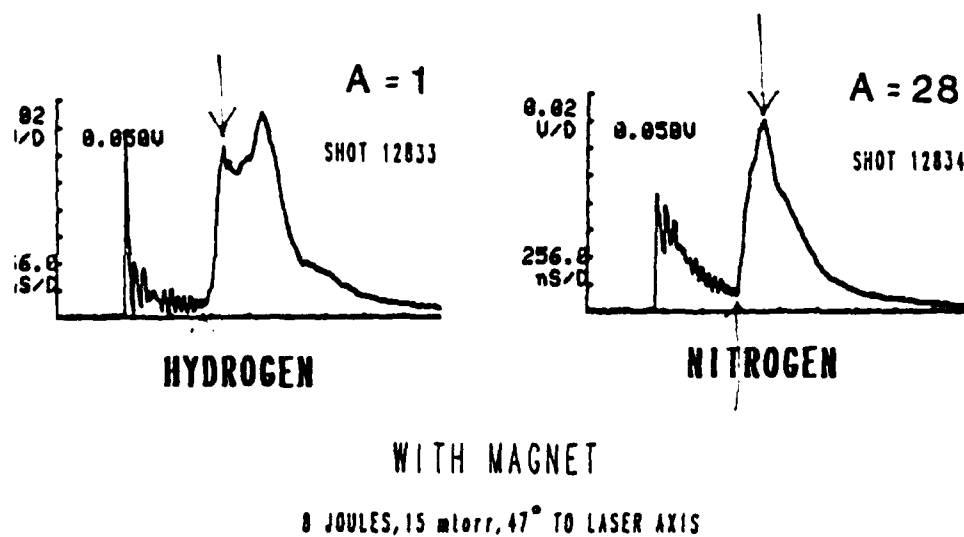


Figure 14. Comparison of debris ion distributions with atomic number of the background gas.

WITH MAGNET

(65° TO LASER AXIS)

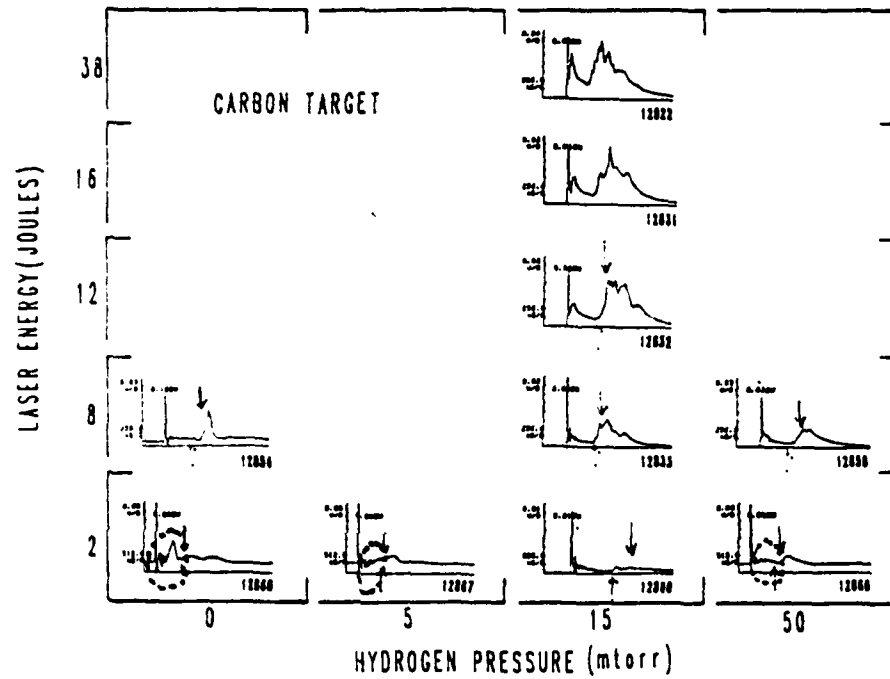


Figure 15. Debris ion time-of-flight signals often show "fast ions" at low laser energy in the presence of a magnetic field.

References

1. J.F. Vesecky et al., JASON Tech. Report #JSR-80-15 (1980). HANE Primer-DNA High Altitude Nuclear Effects Summer Study (to be published 1984).
2. S.T. Kacenjar, B.H. Ripin, J.A. Stamper, J. Grun and E.A. McLean, NRL Memo Report #5260 (1984).
3. J.A. Stamper, B.H. Ripin, E.A. McLean, and S.P. Obenschain, NRL Memo Report #5278 (1984).
4. E.A. McLean, J.A. Stamper, H. Griem, W. Ali, B.H. Ripin, and C.K. Manka, NRL Memo Report #5274 (1984).
5. B.H. Ripin, J.A. Stamper, and E.A. McLean, NRL Memo Report 5279 (1984).
6. C. Prettie (to be published).
7. W. Chesnut, HANE Primer-DNA High Altitude Nuclear Effects Summer Study (to be published 1984).
8. J. Grun, M.H. Emery, M.J. Herbst, S. Kacenjar, C. Opal, E.A. McLean, S.P. Obenschain, and B.H. Ripin (to be published).
9. B.H. Ripin et al., NRL Memo Report #5078 (1983) and in "Laser Interaction and Related Plasma Phenomena," pg. 235-252, ed. H. Hora and G. Miley, Plenum Press (1983).

10. S.T. Kacenjar and C.K. Manka (to be published).
11. M.J. Herbst and J. Grun, Phys. Fluids 24, 1917 (1981); M.J. Herbst et al., NRL Memo Report #4893 (1980) and #5003 (1983); see also, "Laser Interaction and Related Plasma Phenomena," ed. H. Hora and G. Miley, Plenum Press (1983).
12. B.H. Ripin, DNA High-Altitude Nuclear Effects Summer Study (1982); see also HANE Working Group Meeting at NRL on Jan. 25-27 (1983).
13. R.R. Whitlock, M.H. Emery, J.A. Stamper, E.A. McLean, S.P. Obenschain and M.C. Peckerar, (to be published).
14. B.H. Ripin et al., in "Plasma Physics and Controlled Nuclear Fusion Research - 1982," p. 139-154, IAEA, Vienna, Austria (1983).
15. B.H. Ripin et al., Bull. Am. Phys. Soc. 25, 946 (1980).
16. J. Grun, M. Emery, M.J. Herbst, E.A. McLean, S.P. Obenschain, B.H. Ripin, J.A. Stamper, and R.R. Whitlock, NRL Memo Report #4896 (1983).
17. C. Longmire, M. Alme, R. Kilb, and C. Wright, MRC Report #AMRC-R-338 (1981).
18. M. Lampe, W.M. Manheimer, and K. Papadopoulos, NRL Memo Report #3076 (1975).

19. W. Tsai, L. DeRadd, Jr., and R. LeLevier, RDA Report #RDA-TR-125003-001 (1982).
20. R.A. Smith and J.D. Huba, NRL Memo Report #5092 (1983).
21. R. Stellingwerf, C. Longmire, and M. Alme, AMRC-465 (1983).
22. J.L. Sperling, JAYCOR Report #J530-83-102 (1983).
23. R. Decoste and B.H. Ripin, Phys. Rev. Lett. 40, 34 (1978).
24. B.H. Ripin et al., Phys. Fluids 23, 1012 (1980) and 24, 990 (1981).
25. J. Grun et al., Phys. Fluids 26, 588 (1983).

DISTRIBUTION LIST

DEPARTMENT OF DEFENSE

ASSISTANT SECRETARY OF DEFENSE
COMM, CMD, CONT 7 INTELL
WASHINGTON, D.C. 20301

DIRECTOR
COMMAND CONTROL TECHNICAL CENTER
PENTAGON RM BE 685
WASHINGTON, D.C. 20301
O1CY ATTN C-650
O1CY ATTN C-312 R. MASON

DIRECTOR
DEFENSE ADVANCED RSCH PROJ AGENCY
ARCHITECT BUILDING
1400 WILSON BLVD.
ARLINGTON, VA. 22209
O1CY ATTN NUCLEAR MONITORING RESEARCH
O1CY ATTN STRATEGIC TECH OFFICE

DEFENSE COMMUNICATION ENGINEER CENTER
1860 WIEHLE AVENUE
RESTON, VA. 22090
O1CY ATTN CODE R410
O1CY ATTN CODE R812

DEFENSE TECHNICAL INFORMATION CENTER
CAMERON STATION
ALEXANDRIA, VA. 22314
O2CY

DIRECTOR
DEFENSE NUCLEAR AGENCY
WASHINGTON, D.C. 20305
O1CY ATTN STVL
O4CY ATTN TITL
O1CY ATTN DDST
O3CY ATTN RAAE

COMMANDER
FIELD COMMAND
DEFENSE NUCLEAR AGENCY
KIRTLAND, AFB, NM 87115
O1CY ATTN FCPR

DEFENSE NUCLEAR AGENCY
SAO/DNA
BUILDING 20676
KIRTLAND AFB, NM 87115
O1CY D.C. THORNBURG

DIRECTOR
INTERSERVICE NUCLEAR WEAPONS SCHOOL
KIRTLAND AFB, NM 87115
O1CY ATTN DOCUMENT CONTROL

JOINT CHIEFS OF STAFF
WASHINGTON, D.C. 20301
O1CY ATTN J-3 WWMCCS EVALUATION OFFICE

DIRECTOR
JOINT STRAT TGT PLANNING STAFF
OFFUTT AFB
OMAHA, NB 68113
O1CY ATTN JLTW-2
O1CY ATTN JPST G. GOETZ

CHIEF
LIVERMORE DIVISION FLD COMMAND DNA
DEPARTMENT OF DEFENSE
LAWRENCE LIVERMORE LABORATORY
P.O. BOX 808
LIVERMORE, CA 94550
O1CY ATTN FCPRL

COMMANDANT
NATO SCHOOL (SHAPE)
APO NEW YORK 09172
O1CY ATTN U.S. DOCUMENTS OFFICER

UNDER SECY OF DEF FOR RSCH & ENGRG
DEPARTMENT OF DEFENSE
WASHINGTON, D.C. 20301
O1CY ATTN STRATEGIC & SPACE SYSTEMS (OS)

WWMCCS SYSTEM ENGINEERING ORG
WASHINGTON, D.C. 20305
O1CY ATTN R. CRAWFORD

COMMANDER/DIRECTOR
ATMOSPHERIC SCIENCES LABORATORY
U.S. ARMY ELECTRONICS COMMAND
WHITE SANDS MISSILE RANGE, NM 88002
O1CY ATTN DELAS-EO F. NILES

DIRECTOR
BMD ADVANCED TECH CTR
HUNTSVILLE OFFICE
P.O. BOX 150C
HUNTSVILLE, AL 35807
O1CY ATTN ATC-T MELVIN T. CAPPS
O1CY ATTN ATC-O W. DAVIES
O1CY ATTN ATC-R DON RUSS

PROGRAM MANAGER
BMD PROGRAM OFFICE
5001 EISENHOWER AVENUE
ALEXANDRIA, VA 22333
O1CY ATTN DACS-BMT J. SHEA

CHIEF C-E- SERVICES DIVISION
U.S. ARMY COMMUNICATIONS CMD
PENTAGON RM 1B269
WASHINGTON, D.C. 20310
O1CY ATTN C- E-SERVICES DIVISION

COMMANDER
FRADCOM TECHNICAL SUPPORT ACTIVITY
DEPARTMENT OF THE ARMY
FORT MONMOUTH, N.J. 07703
O1CY ATTN DRSEL-NL-RD H. BENNET
O1CY ATTN DRSEL-PL-ENV H. BOMKE
O1CY ATTN J.E. QUIGLEY

COMMANDER
U.S. ARMY COMM-ELEC ENGRG INSTAL AGY
FT. HUACHUCA, AZ 85613
O1CY ATTN CCC-EMEO GEORGE LANE

COMMANDER
U.S. ARMY FOREIGN SCIENCE & TECH CTR
220 7TH STREET, NE
CHARLOTTESVILLE, VA 22901
O1CY ATTN DRXST-SD

COMMANDER
U.S. ARMY MATERIAL DEV & READINESS CMD
5001 EISENHOWER AVENUE
ALEXANDRIA, VA 22333
O1CY ATTN DRCLDC J.A. BENDER

COMMANDER
U.S. ARMY NUCLEAR AND CHEMICAL AGENCY
7500 BACKLICK ROAD
BLDG 2073
SPRINGFIELD, VA 22150
O1CY ATTN LIBRARY

DIRECTOR
U.S. ARMY BALLISTIC RESEARCH LABORATORY
ABERDEEN PROVING GROUND, MD 21005
O1CY ATTN TECH LIBRARY EDWARD BAICY

COMMANDER
U.S. ARMY SATCOM AGENCY
FT. MONMOUTH, NJ 07703
O1CY ATTN DOCUMENT CONTROL

COMMANDER
U.S. ARMY MISSILE INTELLIGENCE AGENCY
REDSTONE ARSENAL, AL 35809
O1CY ATTN JIM GAMBLE

DIRECTOR
U.S. ARMY TRADOC SYSTEMS ANALYSIS ACTIVITY
WHITE SANDS MISSILE RANGE, NM 88002
O1CY ATTN ATAA-SA
O1CY ATTN TCC/F. PAYAN JR.
O1CY ATTN ATTA-TAC LTC J. HESSE

COMMANDER
NAVAL ELECTRONIC SYSTEMS COMMAND
WASHINGTON, D.C. 20360
O1CY ATTN NAVALEX 034 T. HUGHES
O1CY ATTN PME 117
O1CY ATTN PME 117-T
O1CY ATTN CODE 5011

COMMANDING OFFICER
NAVAL INTELLIGENCE SUPPORT CTR
4301 SUITLAND ROAD, BLDG. 5
WASHINGTON, D.C. 20390
O1CY ATTN MR. DUBBIN STIC 12
O1CY ATTN NISC-50
O1CY ATTN CODE 5404 J. GALET

COMMANDER
NAVAL OCEAN SYSTEMS CENTER
SAN DIEGO, CA 92152
O1CY ATTN J. FERGUSON

NAVAL RESEARCH LABORATORY
WASHINGTON, DC 20375

01CY ATTN CODE 4700 S.L. OSSAKOW
26 CYS IF UNCLASS, 1 CY IF CLASS
01CY ATTN CODE 4701 I. VITKOVITSKY
01CY ATTN CODE 4780 J. Huba (10
CYS IF UNCLASS, 1 CY IF CLASS)
01CY ATTN CODE 7500
01CY ATTN CODE 7550
01CY ATTN CODE 7580
01CY ATTN CODE 7551
01CY ATTN CODE 7555
01CY ATTN CODE 4730 E. MCLEAN
01CY ATTN CODE 4108
01CY ATTN CODE 4730 B. RIPIN
20CY ATTN CODE 2628
100CY ATTN CODE 4730

COMMANDER
NAVAL SEA SYSTEMS COMMAND
WASHINGTON, DC 20362
01CY ATTN CAPT R. PITKIN

COMMANDER
NAVAL SPACE SURVEILLANCE SYSTEM
DHALGREN, VA 22448
01CY ATTN CAPT J.H. BURTON

OFFICER-IN-CHARGE
NAVAL SURFACE WEAPONS CENTER
WHITE OAK, SILVER SPRING, MD 20910
01CY ATTN CODE F31

DIRECTOR
STRATEGIC SYSTEMS PROJECT OFFICE
DEPARTMENT OF THE NAVY
WASHINGTON, DC 20376
01CY ATTN NSP-2141
01CY ATTN NSSP-2722 FRED WIMBERLY

COMMANDER
NAVAL SURFACE WEAPONS CENTER
DAHLGREN LABORATORY
DAHLGREN, VA 22448
01CY ATTN CODE DF-14 R. BUTLER

OFFICE OF NAVAL RESEARCH
ARLINGTON, VA 22217
01CY ATTN CODE 465
01CY ATTN CODE 461
01CY ATTN CODE 402
01CY ATTN CODE 420
01CY ATTN CODE 421

COMMANDER
AEROSPACE DEFENSE COMMAND/DC
DEPARTMENT OF THE AIR FORCE
ENT AFB, CO 90812
01CY ATTN DC MR. LONG

COMMANDER AEROSPACE DEFENSE COMMAND/XPD
DEPARTMENT OF THE AIR FORCE
ENT AFB, CO 80912
01CY ATTN XPDQQ
01CY ATTN XP

AIR FORCE GEOPHYSICS LABORATORY
HANSCOM AFB, MA 01731
01CY ATTN OPR HAROLD GARDNER
01CY ATTN LKB KENNETH S.W. CHAMPION
01CY ATTN OPR ALVA T. STAIR
01CY ATTN PHD JURGEN BUCHAU
01CY ATTN PHD JOHN P. MULLEN

AF WEAPONS LABORATORY
KIRTLAND AFB, NM 87117
01CY ATTN SUL
01CY ATTN CA ARTHUR H. GUENTHER
01CY ATTN NTYCE LT. G. KRAJEI

AFTAC
PATRICK AFB, FL 32925
01CY ATTN TF/MAJ WILEY
01CY ATTN TN

AIR FORCE AVIONICS LABORATORY
WRIGHT-PATTERSON AFB, OH 45433
01CY ATTN AAD WADE HUNT
01CY ATTN AAD ALLEN JOHNSON

DEPUTY CHIEF OF STAFF
RESEARCH, DEVELOPMENT, & ACQ
DEPARTMENT OF THE AIR FORCE
WASHINGTON, DC 20030
01CY ATTN AFRDQ

HEADQUARTERS
ELECTRONIC SYSTEMS DIVISION
DEPARTMENT OF THE AIR FORCE
HANSCOM AFB, MA 01731
01CY ATTN J. DEAS

HEADQUARTERS
ELECTRONIC SYSTEMS DIVISION/YSEA
DEPARTMENT OF THE AIR FORCE
HANSCOM AFB, MA 01732
01CY ATTN YSEA

HEADQUARTERS
ELECTRONIC SYSTEMS DIVISION/DC
DEPARTMENT OF THE AIR FORCE
HANSCOM AFB, MA 01731
OICY ATTN DCKC MAJ J.C. CLARK

COMMANDER
FOREIGN TECHNOLOGY DIVISION, AFSC
WRIGHT-PATTERSON AFB, OH 45433
OICY ATTN NICD LIBRARY
OICY ATTN ETD P. BALLARD

COMMANDER
ROME AIR DEVELOPMENT CENTER, AFSC
GRIFFISS AFB, NY 13441
OICY ATTN DOC LIBRARY/TSLD
OICY ATTN OCSE V. COYNE

SAMSO/SZ
POST OFFICE BOX 92960
WORLDWAY POSTAL CENTER
LOS ANGELES, CA 90009
(SPACE DEFENSE SYSTEMS)
OICY ATTN SZJ

STRATEGIC AIR COMMAND/XPFS
OFFUTT AFB, NE 68113
OICY ATTN ADWATE MAJ BRUCE BAUER
OICY ATTN NRT
OICY ATTN DOK CHIEF SCIENTIST

SAMSO/SK
P.O. BOX 92960
WORLDWAY POSTAL CENTER
LOS ANGELES, CA 90009
OICY ATTN SKA (SPACE COMM SYSTEMS)
M. CLAVIN

SAMSO/MN
NORTON AFB, CA 92409
(MINUTEMAN)
OICY ATTN MNL

COMMANDER
ROME AIR DEVELOPMENT CENTER, AFSC
HANSCOM AFB, MA 01731
OICY ATTN EEP A. LORENTZEN

DEPARTMENT OF ENERGY
LIBRARY ROOM G-042
WASHINGTON, D.C. 20545
OICY ATTN DOC CON FOR A. LABOWITZ

DEPARTMENT OF ENERGY
ALBUQUERQUE OPERATIONS OFFICE
P.O. BOX 5400
ALBUQUERQUE, NM 87115
OICY ATTN DOC CON FOR D. SHERWOOD

EG&G, INC.
LOS ALAMOS DIVISION
P.O. BOX 309
LOS ALAMOS, NM 85544
OICY ATTN DOC CON FOR J. BREEDLOVE

UNIVERSITY OF CALIFORNIA
LAWRENCE LIVERMORE LABORATORY
P.O. BOX 808
LIVERMORE, CA 94550
OICY ATTN DOC CON FOR TECH INFO DEPT
OICY ATTN DOC CON FOR L-389 R. OTT
OICY ATTN DOC CON FOR L-31 R. HAGER
OICY ATTN DOC CON FOR L-46 F. SEWARD

LOS ALAMOS NATIONAL LABORATORY
P.O. BOX 1663
LOS ALAMOS, NM 87545
OICY ATTN DOC CON FOR J. WOLCOTT
OICY ATTN DOC CON FOR R.F. TASCHEK
OICY ATTN DOC CON FOR E. JONES
OICY ATTN DOC CON FOR J. MALIK
OICY ATTN DOC CON FOR R. JEFFRIES
OICY ATTN DOC CON FOR J. ZINN
OICY ATTN DOC CON FOR P. KEATON
OICY ATTN DOC CON FOR D. WESTERVELT
OICY ATTN D. SAPPENFIELD

SANDIA LABORATORIES
P.O. BOX 5800
ALBUQUERQUE, NM 87115
OICY ATTN DOC CON FOR W. BROWN
OICY ATTN DOC CON FOR A. THORNBROUGH
OICY ATTN DOC CON FOR T. WRIGHT
OICY ATTN DOC CON FOR D. DAHLGREN
OICY ATTN DOC CON FOR 3141
OICY ATTN DOC CON FOR SPACE PROJECT DIV

SANDIA LABORATORIES
LIVERMORE LABORATORY
P.O. BOX 969
LIVERMORE, CA 94550
OICY ATTN DOC CON FOR B. MURPHEY
OICY ATTN DOC CON FOR T. COOK

OFFICE OF MILITARY APPLICATION
DEPARTMENT OF ENERGY
WASHINGTON, D.C. 20545
OICY ATTN DOC CON DR. YO SONG

OTHER GOVERNMENT

DEPARTMENT OF COMMERCE
NATIONAL BUREAU OF STANDARDS
WASHINGTON, D.C. 20234
OICY (ALL CORRES: ATTN SEC OFFICER FOR)

INSTITUTE FOR TELECOM SCIENCES
NATIONAL TELECOMMUNICATIONS & INFO ADMIN
BOULDER, CO 80303
OICY ATTN A. JEAN (UNCLASS ONLY)
OICY ATTN W. JTLAUT
OICY ATTN D. CROMBIE
OICY ATTN L. BERRY

NATIONAL OCEANIC & ATMOSPHERIC ADMIN
ENVIRONMENTAL RESEARCH LABORATORIES
DEPARTMENT OF COMMERCE
BOULDER, CO 80302
OICY ATTN R. GRUBB
OICY ATTN AERONOMY LAB G. REID

DEPARTMENT OF DEFENSE CONTRACTORS

AEROSPACE CORPORATION
P.O. BOX 92957
LOS ANGELES, CA 90009
OICY ATTN I. GARFUNKEL
OICY ATTN T. SALMI
OICY ATTN V. JOSEPHSON
OICY ATTN S. BOWER
OICY ATTN D. OLSEN

ANALYTICAL SYSTEMS ENGINEERING CORP
5 OLD CONCORD ROAD
BURLINGTON, MA 01803
OICY ATTN RADIO SCIENCES

AUSTIN RESEARCH ASSOC., INC.
1901 RUTLAND DRIVE
AUSTIN, TX 78758
OICY ATTN L. SLOAN
OICY ATTN R. THOMPSON

BERKELEY RESEARCH ASSOCIATES, INC.
P.O. BOX 983
BERKELEY, CA 94701
OICY ATTN J. WORKMAN
OICY ATTN C. PRETTIE
OICY ATTN S. BRECHT

BOEING COMPANY, THE
P.O. BOX 3707
SEATTLE, WA 98124
OICY ATTN G. KEISTER
OICY ATTN D. MURRAY
OICY ATTN G. HALL
OICY ATTN J. KENNEY

CHARLES STARK DRAPER LABORATORY, INC.
555 TECHNOLOGY SQUARE
CAMBRIDGE, MA 02139
OICY ATTN D.B. COX
OICY ATTN J.P. GILMORE

COMSAT LABORATORIES
LINTHICUM ROAD
CLARKSBURG, MD 20734
OICY ATTN G. HYDE

CORNELL UNIVERSITY
DEPARTMENT OF ELECTRICAL ENGINEERING
ITHACA, NY 14850
OICY ATTN D.T. FARLEY, JR.

ELECTROSPACE SYSTEMS, INC.
BOX 1359
RICHARDSON, TX 75080
OICY ATTN H. LOGSTON
OICY ATTN SECURITY (PAUL PHILLIPS)

EOS TECHNOLOGIES, INC.
606 Wilshire Blvd.
Santa Monica, Calif 90401
OICY ATTN C.B. GABBARD

ESL, INC.
495 JAVA DRIVE
SUNNYVALE, CA 94086
OICY ATTN J. ROBERTS
OICY ATTN JAMES MARSHALL

GENERAL ELECTRIC COMPANY
SPACE DIVISION
VALLEY FORGE SPACE CENTER
GODDARD BLVD KING OF PRUSSIA
P.O. BOX 8555
PHILADELPHIA, PA 19101
OICY ATTN M.H. BORTNER SPACE SCI LAB

GENERAL ELECTRIC COMPANY
P.O. BOX 1122
SYRACUSE, NY 13201
OICY ATTN F. REIBERT

GENERAL ELECTRIC TECH SERVICES CO., INC.
HMS
COURT STREET
SYRACUSE, NY 13201
OICY ATTN G. MILLMAN

GEOPHYSICAL INSTITUTE
UNIVERSITY OF ALASKA
FAIRBANKS, AK 99701
(ALL CLASS ATTN: SECURITY OFFICER)
OICY ATTN T.M. DAVIS (UNCLASS ONLY)
OICY ATTN TECHNICAL LIBRARY
OICY ATTN NEAL BROWN (UNCLASS ONLY)

GTE SYLVANIA, INC.
ELECTRONICS SYSTEMS GRP-EASTERN DIV
77 A STREET
NEEDHAM, MA 02194
OICY ATTN DICK STEINHOFF

HSS, INC.
2 ALFRED CIRCLE
BEDFORD, MA 01730
OICY ATTN DONALD HANSEN

ILLINOIS, UNIVERSITY OF
107 COBLE HALL
150 DAVENPORT HOUSE
CHAMPAIGN, IL 61820
(ALL CORRES ATTN DAN MCCLELLAND)
OICY ATTN K. YEH

INSTITUTE FOR DEFENSE ANALYSES
1801 NO. BEAUREGARD STREET
ALEXANDRIA, VA 22311
OICY ATTN J.M. AELN
OICY ATTN ERNEST BAUER
OICY ATTN HANS WOLFARD
OICY ATTN JOEL BENGSTON

INTL TEL & TELEGRAPH CORPORATION
500 WASHINGTON AVENUE
NUTLEY, NJ 07110
OICY ATTN TECHNICAL LIBRARY

JAYCOR
11011 TORREYANA ROAD
P.O. BOX 85154
SAN DIEGO, CA 92138
OICY ATTN J.L. SPERLING

JOHNS HOPKINS UNIVERSITY
APPLIED PHYSICS LABORATORY
JOHNS HOPKINS ROAD
LAUREL, MD 20810
OICY ATTN DOCUMENT LIBRARIAN
OICY ATTN THOMAS POTEIRA
OICY ATTN JOHN DASSOULAS

KAMAN SCIENCES CORP
P.O. BOX 7461
COLORADO SPRINGS, CO 80933
OICY ATTN T. MEAGHER

KAMAN TEMPO-CENTER FOR ADVANCED STUDIES
816 STATE STREET (P.O. DRAWER QQ)
SANTA BARBARA, CA 93102
OICY ATTN DASIAC
OICY ATTN WARREN S. KNAPP
OICY ATTN WILLIAM MCNAMARA
OICY ATTN E. GAMBILL

LINKABIT CORP
10453 ROSELLE
SAN DIEGO, CA 92121
OICY ATTN IRWIN JACOBS

LOCKHEED MISSILES & SPACE CO., INC
P.O. BOX 504
SUNNYVALE, CA 94088
OICY ATTN DEPT 60-12
OICY ATTN D.R. CHURCHILL

LOCKHEED MISSILES & SPACE CO., INC.
3251 HANOVER STREET
PALO ALTO, CA 94304
OICY ATTN MARTIN WALT DEPT 52-12
OICY ATTN W.L. IMHOF DEPT 52-12
OICY ATTN RICHARD G. JOHNSON DEPT 52-12
OICY ATTN J.B. CLADIS DEPT 52-12

MARTIN MARIETTA CORP
ORLANDO DIVISION
P.O. BOX 5837
ORLANDO, FL 32805
OICY ATTN R. HEFFNER

M.I.T. LINCOLN LABORATORY
P.O. BOX 73
LEXINGTON, MA 02173
OICY ATTN DAVID M. TOWLE
OICY ATTN L. LOUGHLIN
OICY ATTN D. CLARK

MCDONNELL DOUGLAS CORPORATION
5301 BOLSA AVENUE
HUNTINGTON BEACH, CA 92647
O1CY ATTN N. HARRIS
O1CY ATTN J. MOULE
O1CY ATTN GEORGE MROZ
O1CY ATTN W. OLSON
O1CY ATTN R.W. HALPRIN
O1CY ATTN TECHNICAL LIBRARY SERVICES

MISSION RESEARCH CORPORATION
735 STATE STREET
SANTA BARBARA, CA 93101
O1CY ATTN P. FISCHER
O1CY ATTN W.F. CREVIER
O1CY ATTN STEVEN L. GUTSCHE
O1CY ATTN R. BOGUSCH
O1CY ATTN R. HENDRICK
O1CY ATTN RALPH KILB
O1CY ATTN DAVE SOWLE
O1CY ATTN F. FAJEN
O1CY ATTN M. SCHEISE
O1CY ATTN CONRAD L. LONGMIRE
O1CY ATTN B. WHITE

MISSION RESEARCH CORP.
1720 RANDOLPH ROAD, S.E.
ALBUQUERQUE, NEW MEXICO 87106
O1CY R. STELLINGWERF
O1CY M. ALME
O1CY L. WRIGHT

MITRE CORPORATION, THE
P.O. BOX 208
BEDFORD, MA 01730
O1CY ATTN JOHN MORGANSTERN
O1CY ATTN G. HARDING
O1CY ATTN C.E. CALLAHAN

MITRE CORP
WESTGATE RESEARCH PARK
1820 DOLLY MADISON BLVD
MCLEAN, VA 22101
O1CY ATTN W. HALL
O1CY ATTN W. FOSTER

PACIFIC-SIERRA RESEARCH CORP
12340 SANTA MONICA BLVD.
LOS ANGELES, CA 90025
O1CY ATTN E.C. FIELD, JR.

PENNSYLVANIA STATE UNIVERSITY
IONOSPHERE RESEARCH LAB
318 ELECTRICAL ENGINEERING EAST
UNIVERSITY PARK, PA 16802
(NO CLASS TO THIS ADDRESS)
O1CY ATTN IONOSPHERIC RESEARCH LAB

PHOTOMETRICS, INC.
4 ARROW DRIVE
WOBURN, MA 01801
O1CY ATTN IRVING L. KOFSKY

PHYSICAL DYNAMICS, INC.
P.O. BOX 3027
BELLEVUE, WA 98009
O1CY ATTN E.J. FREMOUN

PHYSICAL DYNAMICS, INC.
P.O. BOX 10367
OAKLAND, CA 94610
ATTN A. THOMSON

R & D ASSOCIATES
P.O. BOX 9695
MARINA DEL REY, CA 90291
O1CY ATTN FORREST GILMORE
O1CY ATTN WILLIAM B. WRIGHT, JR.
O1CY ATTN ROBERT F. LELEVIER
O1CY ATTN WILLIAM J. KARZAS
O1CY ATTN H. ORY
O1CY ATTN C. MACDONALD
O1CY ATTN R. TURCO
O1CY ATTN L. DeRAND
O1CY ATTN W. TSAI

RAND CORPORATION, THE
1700 MAIN STREET
SANTA MONICA, CA 90406
O1CY ATTN CULLEN CRAIN
O1CY ATTN ED BEDROZIAN

RAYTHEON CO.
528 BOSTON POST ROAD
SUDBURY, MA 01776
O1CY ATTN BARBARA ADAMS

RIVERSIDE RESEARCH INSTITUTE
330 WEST 42nd STREET
NEW YORK, NY 10036
O1CY ATTN VINCE TRAPANI

SCIENCE APPLICATIONS, INC.
1150' PROSPECT PLAZA
LA JOLLA, CA 92037
01CY ATTN LEWIS M. LINSON
01CY ATTN DANIEL A. HAMLIN
01CY ATTN E. FRIEMAN
01CY ATTN E.A. STRAKER
01CY ATTN CURTIS A. SMITH
01CY ATTN JACK MCDUGALL

SCIENCE APPLICATIONS, INC
1710 GOODRIDGE DR.
MCLEAN, VA 22102
ATTN: J. COCKAYNE

SRI INTERNATIONAL
333 RAVENSWOOD AVENUE
MENLO PARK, CA 94025
01CY ATTN DONALD NEILSON
01CY ATTN ALAN BURNS
01CY ATTN G. SMITH
01CY ATTN R. TSUNODA
01CY ATTN DAVID A. JOHNSON
01CY ATTN WALTER G. CHESNUT
01CY ATTN CHARLES L. RINO
01CY ATTN WALTER JAYE
01CY ATTN J. VICKREY
01CY ATTN RAY L. LEADABRAND
01CY ATTN G. CARPENTER
01CY ATTN G. PRICE
01CY ATTN R. LIVINGSTON
01CY ATTN V. GONZALES
01CY ATTN D. MCDANIEL

TECHNOLOGY INTERNATIONAL CORP
75 WIGGINS AVENUE
BEDFORD, MA 01730
01CY ATTN W.P. BOQUIST

TOYON RESEARCH CO.
P.O. Box 6890
SANTA BARBARA, CA 93111
01CY ATTN JOHN ISE, JR.
01CY ATTN JOEL GARBARINO

TRW DEFENSE & SPACE SYS GROUP
ONE SPACE PARK
REDONDO BEACH, CA 90273
01CY ATTN R. K. PLEBUCH
01CY ATTN S. ALTSCHULER
01CY ATTN D. DEE
01CY ATTN D/ STOCKWELL
SNTF/1575

VISIDYNE
SOUTH BEDFORD STREET
BURLINGTON, MASS 01803
01CY ATTN W. REIDY
01CY ATTN J. CARPENTER
01CY ATTN C. HUMPHREY

DATE
FILME